CrossMark

ORIGINAL CONTRIBUTION

Vesicle aggregation based on hydrophobic interactions

Jian-xi Zhao[1] · **Fen Liu**[1] · **Dan-hua Xie**[1]

Abstract Vesicles were formed in aqueous mixtures of gemini anionic surfactant, O,O′-bis(sodium 2-alkylcarboxylate)-p-dibenzenediol (referred to as $C_m\phi_2C_m$, m=10, 12), and single-chain cationic surfactant, alkyltrimethylammonium bromides C_nNBr (n=8, 10, 12). This was confirmed by measurements of solution turbidity, dynamic light scattering (DLS) and freeze-fractured TEM. The improvement of the $C_m\phi_2C_m$ molecular geometry by C_nNBr was considered to have been due to vesicle formation. As the temperature was raised, these vesicles were found to associate together and DLS measurements showed a rapid increase of the aggregate size at the critical temperature T_c. The mechanism of vesicle aggregation was assumed to be due to the temperature-induced configuration transition of a few $C_m\phi_2C_m$ molecules in the vesicles from *cis*- into *trans*-form. Thus, a few tails of $C_m\phi_2C_m$ stretched toward the solution. When the vesicles approached, these projecting tails interacted hydrophobically, thereby noncovalently attaching one vesicle to another. This should benefit from the special molecular structure of $C_m\phi_2C_m$ with a long, rigid spacer.

Keywords Gemini surfactant · Vesicle formation · Vesicle aggregation · Hydrophobic interaction

✉ Jian-xi Zhao
jxzhao.colloid@fzu.edu.cn

1 Institute of Colloid and Interface Chemistry, College of Chemistry and Chemical Engineering, Fuzhou University, Fuzhou, Fujian 350108, People's Republic of China

Introduction

Vesicle aggregation has attracted much interest in the past few decades because of its applications in the modelling of biomembranes [1–3] and in drug and gene delivery [4, 5]. It is known that the change of some experimental conditions can induce the aggregation of vesicles, for example, surfactant composition [6, 7], external additives [8–13], solution pH values [11, 14, 15], temperature [11, 16, 17], etc. In these cases, the reduction, electrostatic interaction or ionic complex formation was considered to be the main mechanism of vesicle aggregation. Besides, Huang et al. assumed inter-vesicular hydrophobic interaction among the exposed hydrophobic part of the surfactant head groups as the driving force for vesicle aggregation in the catanionic surfactant system of sodium n-dodecylsulfate/n-dodecyltributylammonium bromide [16, 17]. In this system, the extended butyl groups on the surface of the vesicles provide such a hydrophobic force as to catch other butyls on another vesicle and bring them together. They further confirmed that the shorter groups such as methyls, ethyls or propyls carried by cationic surfactants cannot achieve this [16]. Another more interesting system utilising hydrophobic interaction to link vesicles was reported by Menger and Peresypkin [18]. In their system, the vesicle was constructed by asymmetric gemini surfactants that consisted of phosphate and quaternary ammonium head groups, a two-carbon spacer, and two hydrophobic tails of different lengths (abbreviated as C_m-C_n, where m and n are the number of carbon atoms on each tail, respectively). They found that some vesicles were cohesive, which was conceptualised as having a "pearls on a string" morphology. This phenomenon was interpreted as owing to the protrusion of short chains from the vesicle surfaces; it thereby created
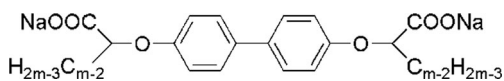
Scheme 1 Chemical structure of $C_m\phi_2C_m$

the opportunity to link neighbouring vesicles through the hydrophobic interactions between the extended short chains. This approach might be considerably more effective when associating the neighbouring vesicles, by which those strings of vesicles may form a complex three-dimensional network, thus making the solution very viscous.

Here, we report a new system of vesicle aggregation, based upon the hydrophobic effect, in which the vesicles were formed by mixed anionic gemini surfactant, O,O′-bis(sodium 2-alkylcarboxylate)-p-dibenzenediol (referred to as $C_m\phi_2C_m$, Scheme 1), and cationic single-chain surfactant, alkyltrimethylammonium bromides C_nNBr. Here, $C_m\phi_2C_m$ was a family of the gemini surfactants and its molecule carried a long, rigid spacer between the two head groups. This molecular structure made its two tails difficult to be brought into close mutual proximity and yielded a pseudo volume between them. Thus, $C_m\phi_2C_m$ had a columnar-like molecular geometry and favoured the formation of aggregates with low surface curvature [19]. We have obtained threadlike micelles by using $C_m\phi_2C_m$ [20] and hoped that they would form vesicles under certain conditions. Besides, the long, rigid spacer of $C_m\phi_2C_m$ made its two tails possibly extend in opposite directions, i.e., in a *trans*-configuration. This could form novel network aggregates through the interactions between the extending alkyl tails [21]. As mentioned, Menger and Peresypkin have linked the vesicles formed by C_m-C_n with the interactions between their extending short tails [18]. Thus, the $C_m\phi_2C_m$ was also expected to create a new case of vesicle aggregation based on its *trans*-configuration.

Experimental

Materials

The carboxylate gemini surfactants, $C_{12}\phi_2C_{12}$ and $C_{10}\phi_2C_{10}$, were synthesised in our laboratory [21]. Octyl-, decyl- and dodecyl-trimethylammonium bromides (denoted as C_8NBr, $C_{10}NBr$ and $C_{12}NBr$, respectively) were purchased from Acros at a purity of 98 %. 1,6-Diphenyl-1,3,5-hexatriene (DPH) was sourced from Aldrich and used as a hydrophobic probe. All solutions were prepared with Milli-Q water with a resistivity of 18.2 MΩ·cm.

Methods

Turbidity Turbidity of the solutions was measured with a UV/vis spectrophotometer (Hitach U-3010, Japan) equipped with a thermostat cell holder and a magnetic stirring device, using quartz cells of 1-cm path length. Transmittance at 500 nm, where the surfactants had no absorption, was recorded to characterise the turbidity.

Dynamic light scattering Dynamic light scattering of micellar solutions was measured with a Brookhaven Instrument which comprised a BI-200SM goniometer, a BI-9000AT digital correlator (522 channels) and a photomultiplier detector. A green laser with an output power of 200 mW and a wavelength of 532 nm was used as the light source. The measurement temperature was controlled by a thermostatic circulator (Poly-science, USA) with an accuracy ±0.01 °C. All solutions were filtered through 0.22-μm Millipore filters into cylindrical light-scattering cells (external diameter, 25 mm). The experimental data were analysed by the CONTIN program to get the intensity-fraction distributions around each characteristic aggregate size.

Fig. 1 Turbidity as a function of β for $C_{12}\phi_2C_{12}$(10 mmol L^{-1})/C_nNBr (**a**) and $C_{10}\phi_2C_{10}$ (10 mmol L^{-1})/C_nNBr (**b**) systems at 25 °C, in which the onset for an abrupt decrease in transmittance is denoted as the critical β_v to indicate vesicle formation
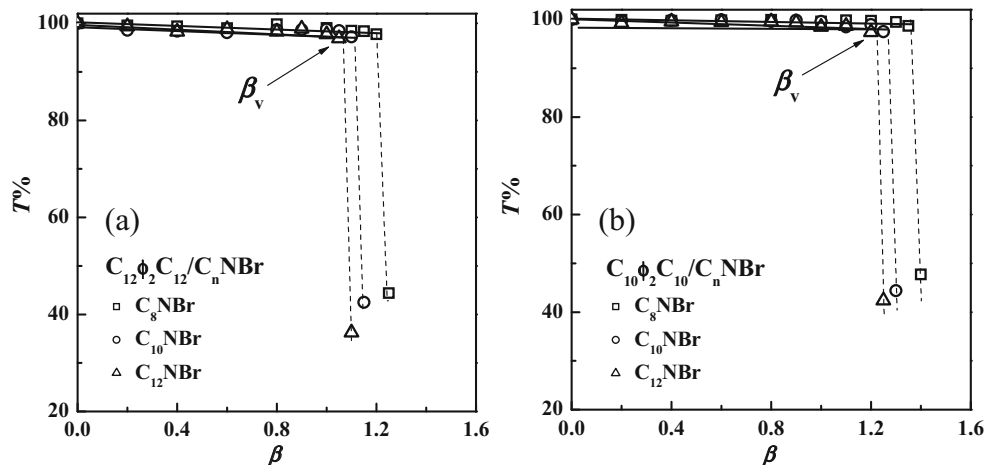
Table 1 Values of β_v

β_v	C_8NBr	$C_{10}NBr$	$C_{12}NBr$
$C_{12}\phi_2C_{12}$ with	1.20 (1.32)	1.10 (1.01)	1.05 (0.864)
$C_{10}\phi_2C_{10}$ with	1.35 (1.58)	1.25 (1.33)	1.20 (1.03)

The data in parentheses are from Fig. 4, indicating the onset of a suitable molecular geometry

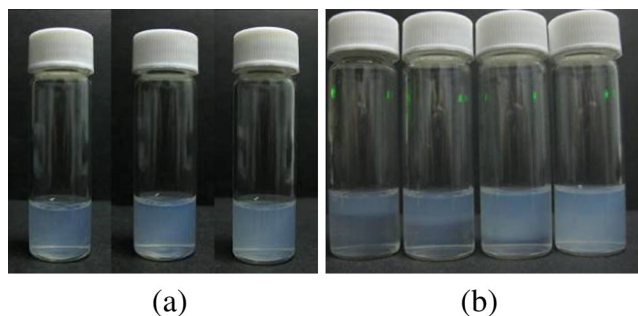(a)　　　　　　　　　(b)

Fig. 2 **a** Appearance of $C_{12}\phi_2C_{12}$ (10 mmol L^{-1})/C_nNB solutions at $\beta=$ 1.6 and 25 °C: from *left* to *right*, $n=8$, 10 and 12. **b** Two aqueous phases (ASTP) of $C_{12}\phi_2C_{12}$ (10 mmol L^{-1})/C_8NBr as an example: from *left* to *right*, $\beta=1.25$, 1.30, 1.325 and 1.35

Freeze-fractured TEM The solution for the test was put into a 25±0.1 °C water bath for at least 1 h. Then, a small amount of solution was coated onto a 0.1-mm-thick gold disc. The sample was rapidly frozen by plunging it into liquid nitrogen cooled liquid ethane. After a few seconds, the sample was transferred onto a specimen holder immersed in liquid nitrogen and then put into the freeze-etching apparatus (Bal-tec, BALZERS BAF-400D, Liechtenstein). The fracturing and replication process was performed at a temperature of −165 °C and at a pressure of 2×10^{-6} mbar. The sample was replicated with 10 nm carbon at an angle of 90° and then 2 nm Pt at an angle of 45°. After that, acetone/dilute sodium hydroxide solution was used to remove the soluble component to obtain the replica which was then examined with a Philips TECHAI 20 transmission electron microscope.
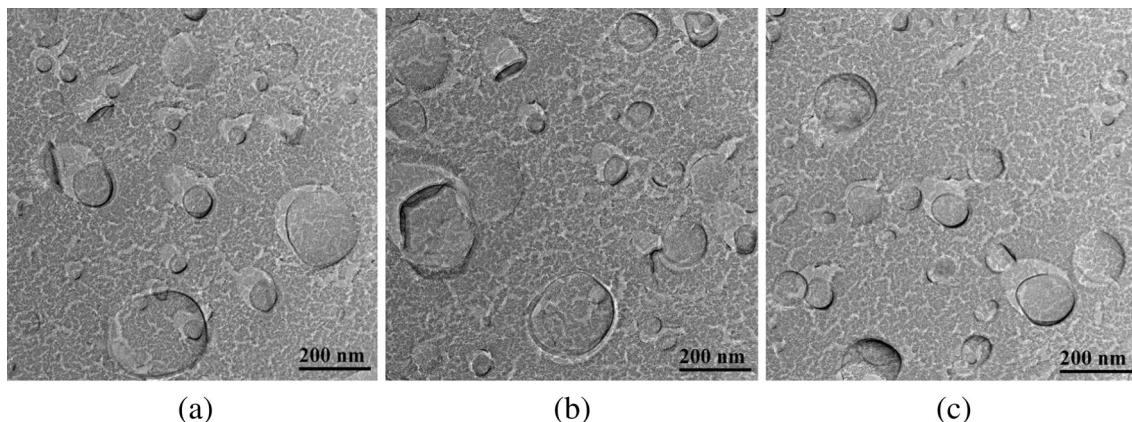
Results and discussion

Vesicle formation with assistance of C_nNBr

Figure 1 shows the solution turbidity expressed as transmittance ($T\%$) at 500 nm as a function of the mole ratio of C_nNB to $C_m\phi_2C_m$ (β), in which the critical point inducing a rapid fall in $T\%$ was denoted as β_v (Table 1). The appearance (in photographs) of some typical $C_{12}\phi_2C_{12}$/C_nNB solutions is shown in Fig. 2, in which the two aqueous phases (ASTP) can be seen in some examples. All of these indicated vesicle formation, which was further confirmed by the FF-TEM images (Fig. 3).

The mechanism of vesicle formation can be interpreted as an effective gemini molecular geometry improved by the addition of C_nNB. Israelachvili et al. suggested the dimensionless packing parameter P as an index to predict the shape and size of the aggregates [22]. This parameter reflects the effective molecular geometry of a given surfactant molecule and is defined as $P=v/(al)$ where v is the hydrocarbon chain volume, a is the optimum head group area *per* molecule and l is the hydrocarbon chain length. Vesicles are favoured when $0.5< P<1$ [22].

For the present systems, it was supposed that all the added C_nNBr associated with $C_{12}\phi_2C_{12}$ or $C_{10}\phi_2C_{10}$ to form vesicles under strong electrostatic attraction. In the mixed vesicles, two moieties coexisted, i.e., the ion pairs consisted of two C_nNBr with one gemini and residual single $C_{12}\phi_2C_{12}$ or $C_{10}\phi_2C_{10}$. Thus, the effective packing parameter P_{eff} can be estimated by (1) [23]:

$$P_{eff} = \left(v/a_0 l\right)_{eff} = x_1 P_{ion\ pairs} + x_2 P_{gemini} \tag{1}$$

where x_1 and x_2 are the mole fractions of the ion pairs and the single gemini, respectively, in the aggregate.

Figure 4 shows the linear variation of P_{eff} with β for all systems analysed here. The horizontal dashed line indicated the theoretical boundary above which vesicles could have been formed. The crossovers between the P_{eff} plots and the

(a)　　　　　　　　　(b)　　　　　　　　　(c)

Fig. 3 FF-TEM images of **a** $C_{12}\phi_2C_{12}$ (10 mmol L^{-1})/$C_{12}NBr$, **b** $C_{12}\phi_2C_{12}$ (10 mmol L^{-1})/C_8NBr and **c** $C_{10}\phi_2C_{10}$ (10 mmol L^{-1})/C_8NBr at $\beta=1.6$
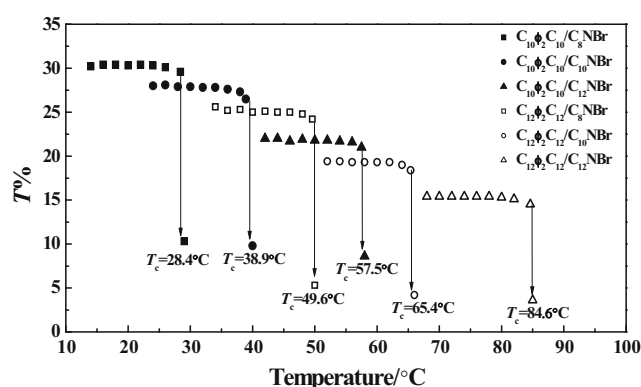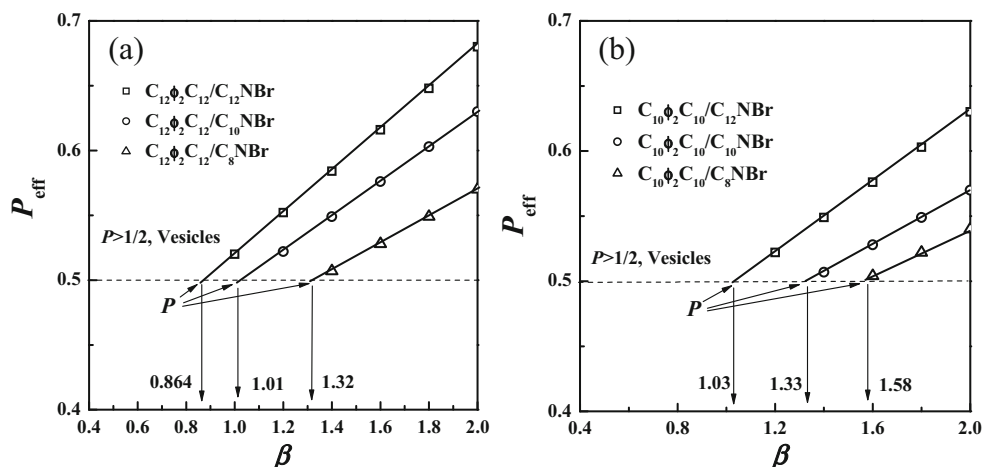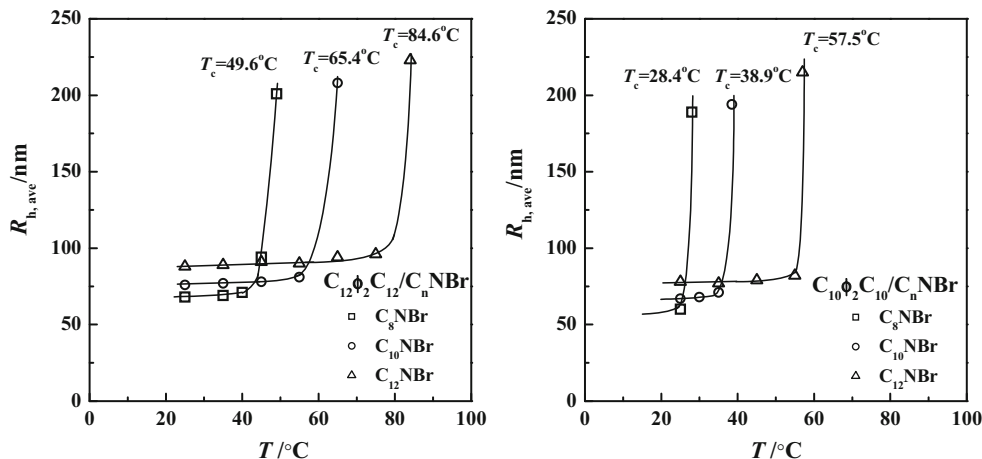
Fig. 5 Turbidity (expressed as transmittance at 500 nm) curves for the mixed systems at $\beta=1.6$ under heating, in which *arrows* show the critical temperature to clouding (T_c)

horizontal dashed line indicated the critical β values required to form vesicles for each system. These values listed in parentheses in Table 1 were consistent with those experimental points (β_V). This mechanism dominated the improvement of the effective molecular geometry was the main reason for vesicle formation.

Vesicle aggregation at high temperatures

Figure 5 shows the solution turbidity (expressed as transmittance at 500 nm) as a function of temperature for the $C_{12}\phi_2C_{12}/C_nNBr$ and $C_{10}\phi_2C_{10}/C_nNBr$ systems at $\beta=1.6$. As the temperature increased, the solutions became cloudy at a critical temperature (T_c) which was indicated by an arrow for each system. The dynamic light scattering (DLS) measurements showed a rapid increase in aggregate size when the temperature approached T_c (Fig. 6). All these indicated that the vesicles associated at high temperatures.

Mechanism of vesicle aggregation

To understand the mechanism of vesicle aggregation, one detail was important: what was the attractive force to pull neighbouring vesicles together in the present case? According to the characteristics of the $C_m\phi_2C_m$ molecular structure, it was believed that this responsibility should be borne by the alkyl tails themselves. As expounded in "Introduction"
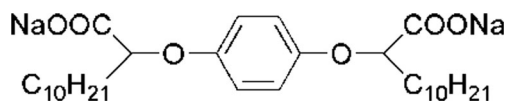
Fig. 6 Variation of average hydrodynamic radius ($R_{h,ave}$) with temperature for $C_{12}\phi_2C_{12}/C_nNBr$ (left) and $C_{10}\phi_2C_{10}/C_nNBr$ (right) systems at $\beta=1.6$

Fig. 7 Schematic representation of bridging between neighbouring vesicles by the extension of the alkyl tails of $C_m\phi_2C_m$
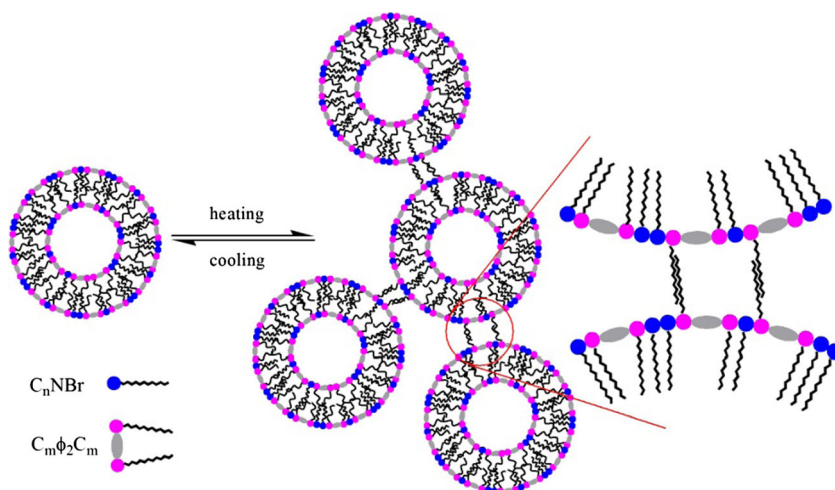
section, $C_m\phi_2C_m$ has a long and rigid spacer in its molecular structure, which made its two alkyl tails able to produce both *cis*- and *trans*-configurations, i.e., toward the same or the opposite side. When $C_m\phi_2C_m$ formed the vesicles together with C_nNBr, it should prefer the *cis*-configuration so as to make the tails penetrate the inner of the double layer of vesicles. However, this cannot guarantee that all of the $C_m\phi_2C_m$ molecules always kept one kind of configuration. When temperature was raised, the action of the alkyl tails was enhanced. A few molecules probably adopted *trans*-configurations and stretched one tail toward the solution. When the vesicles approached each other in solution, those projecting tails associated hydrophobically, thereby non-covalently attaching one vesicle to another (Fig. 7). This was perhaps the mechanism underpinning the present vesicle aggregation.

A similar effect was suggested by Menger and Peresypkin [18], in which they studied the vesicles generated by a set of zwitterionic geminis with two alkyl tails of different lengths (these geminis had general structure: $ROPO_2$-$OCH_2CH_2N^+(CH_3)_2R'$, where R and R′ were hydrocarbon chains and were referred to as C_m-C_n). They obtained strings of vesicles for those zwitterionic geminis with highly asymmetric alkyl tails such as C_{14}-C_8, C_{18}-C_7, C_{22}-C_6, etc., using the short chains extending from the vesicles to associate with the projecting chains of neighbouring vesicles. In this system, the two alkyl tails of $C_m\phi_2C_m$ had the same length, and thereby, it may have been relatively difficult to extend one tail compared with the cases described by Menger and Peresypkin. This may have been why the present vesicle aggregation occurred at higher temperatures.

It was of significance to compare the present cases with those generated by the homologue of $C_{12}\phi C_{12}$, O,O′-

bis(sodium 2-dodecylcarboxylate)-*p*-benzenediol (generally referred to as $C_{12}\phi C_{12}$, Scheme 2). Compared with $C_{12}\phi_2C_{12}$, $C_{12}\phi C_{12}$ has a shorter spacer but can also form vesicles together with C_nNBr, which resulted in two aqueous phases (ASTP) [24, 25]. Figure 8 shows the variation of average hydrodynamic radius ($R_{h,ave}$) of the vesicles formed by $C_{12}\phi C_{12}/C_8NBr$ at $\beta=1.6$ with temperature. It was found that $R_{h,ave}$ remained practically constant over a wide range of temperatures, indicating no vesicle aggregation in the case of $C_{12}\phi C_{12}/C_8NBr$. This result indicated that responsibility for extending the tail out to the vesicle was indeed borne by $C_m\phi_2C_m$ in the present cases, which agreed with the special property of these geminis having both *cis*- or *trans*-configuration as mentioned.

Figure 9 shows the influence of the hydrophobic interaction between the alkyl tails on T_c. As seen in Fig. 9, the stronger the hydrophobic interaction (which was a result of the longer alkyl tails), the lower the value of T_c. This clearly

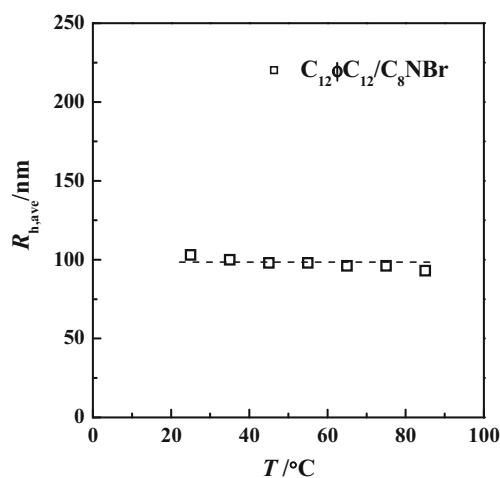**Scheme 2** Chemical structure of $C_{12}\phi C_{12}$

Fig. 8 Variation of average hydrodynamic radius ($R_{h,ave}$) of the vesicles with temperature for a $C_{12}\phi C_{12}/C_8NBr$ system at $\beta=1.6$
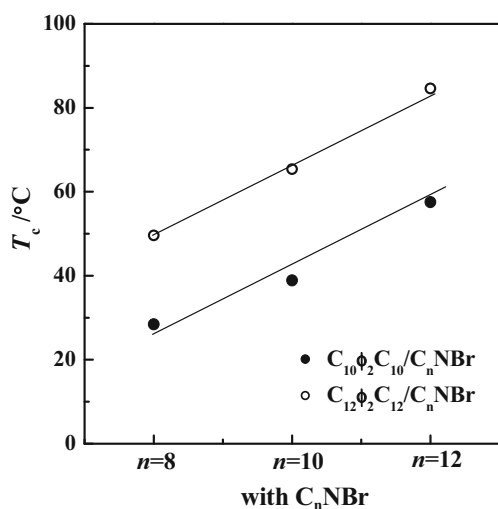
Fig. 9 T_c-dependence on the alkyl tail length of C_nNBr

indicated that a hydrophobic interaction existed between the alkyl tails and strongly influenced vesicle aggregation. If the mechanism of vesicle aggregation was indeed due to the *trans*-configuration of some $C_{12}\phi_2C_{12}$ or $C_{10}\phi_2C_{10}$, the result shown in Fig. 9 supported this mechanism because the strong hydrophobic interaction hindered the extension of the alkyl tail of $C_m\phi_2C_m$.

Effect of vesicle surface charge

Figure 10 shows the effect of the mole ratio of C_nNBr to gemini surfactants (β) on T_c, in which T_c decreased with increasing β. The increase in β meant that more C_nNBr molecules entered the mixed vesicles and this neutralised the charge thereof and reduces the repulsion between them. As a result, the aggregation of vesicles was promoted and T_c decreased. The addition of NaBr also yielded a similar effect (Fig. 11) because the salt screened the surface charge on the vesicles. The two approaches can provide methods of adjusting the intensity of vesicle aggregation, which may be useful in future applications.

Fig. 10 Effect of β on T_c for $C_{12}\phi_2C_{12}/C_nNBr$ (*left*) and $C_{10}\phi_2C_{10}/C_nNBr$ (*right*) systems
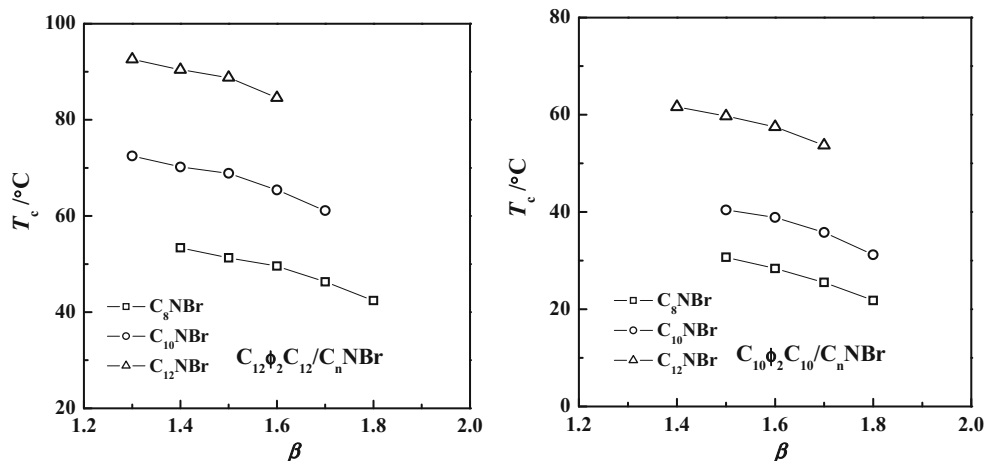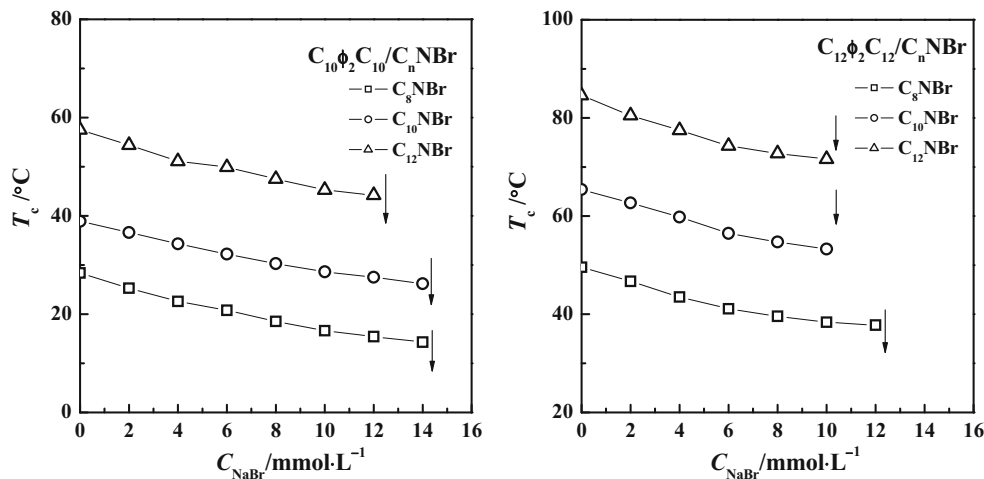

Fig. 11 Effect of NaBr concentration on T_c for $C_{12}\phi_2C_{12}/C_nNBr$ (*left*) and $C_{10}\phi_2C_{10}/C_nNBr$ (*right*) systems at $\beta=1.6$ (*Arrows* indicate precipitation)

Conclusion

The carboxylate gemini surfactant $C_m\phi_2C_m$ exhibited novel self-assembly behaviour, which benefitted from its special molecular structure. $C_m\phi_2C_m$ carried a long, rigid spacer that made its two alkyl tails difficult to bring into close proximity. This had two effects: firstly, $C_m\phi_2C_m$ had a columnar-like molecular geometry, which was the origin of the formation of the vesicles together with C_nNBr, and secondly, the $C_m\phi_2$-C_m molecule could rotate its two alkyl tails freely, i.e., adopting either *cis*- or *trans*-configurations, which led to the present vesicle aggregation and may also hold a function which produced this novel self-assembly behaviour. All of these aspects indicated that the gemini surfactants, with their long, rigid spacers, were good candidates for novel self-assemblies and further applications.

References

1. Casal HL, Mantsch HH, Hauser H (1987) Infrared studies of fully hydrated saturated phosphatidylserine bilayers. Effect of lithium and calcium. Biochemistry 26:4408–4416
2. Streefland L, Wagenaar A, Hoekstra D, Engberts JBFN (1993) Effect of alkyl chain asymmetry on the fusion and crystallization behavior of vesicles formed from di-n-alkyl phosphates. Langmuir 9:219–222
3. Ravoo BJ, Engberts JBFN (2001) Vesicles formed from phospholipid analogues containing an oligomerisable head group. Properties and mechanism of fusion. J Chem Soc Perkin Trans 2: 1869–1886
4. Collins D, Litzinger DC, Huang L (1990) Structural and functional comparisons of pH-sensitive liposomes composed of phosphatidylethanolamine and three different diacylsuccinylglycerols. Biochim Biophys Acta 1025:234–242
5. Guo X, Szoka FC (2003) Chemical approaches to triggerable lipid vesicles for drug and gene delivery. Acc Chem Res 36:335–341
6. Walker SA, Zasadzinski JA (1997) Electrostatic control of spontaneous vesicle aggregation. Langmuir 13:5076–5081
7. Visscher I, Engberts JBFN (2000) Vesicles of mixtures of the bolaform amphiphile sodium Di-n-decyl α,ω-eicosanyl bisphosphate and sodium di-n-decyl phosphate. Langmuir 16:52–58
8. Minami H, Inoue T (1999) Aggregation of dipalmitoylphosphatidylcholine vesicles induced by some metal ions with high activity for hydrolysis. Langmuir 15:6643–6651
9. Menger FM, Balachander N (1992) Chemically-induced aggregation, budding, and fusion in giant vesicles: direct observation by light microscopy. J Am Chem Soc 114:5862–5863
10. Menger FM, Gabrielson K (1994) Chemically-induced birthing and foraging in vesicle systems. J Am Chem Soc 116:1567–1568
11. Yao J, Feng Y, Zhao Y, Li Z, Huang J, Fu H (2007) Vesicle aggregation in aqueous mixtures of negatively charged polyelectrolyte and conventional cationic surfactant. J Colloid Interface Sci 314: 523–530
12. Moyuhas D, Nir S, Lichtenberg D (1996) Aggregation of phospholipid vesicles by water-soluble polymers. Biophys J 71:2602–2612
13. Sommerdijk NAJM, Hoeks THL, Synak M, Feiters MC, Nolte RJM, Zwanenburg B (1997) Stereodependent fusion and fission of vesicles: calcium binding of synthetic gemini phospholipids containing two phosphate groups. J Am Chem Soc 119:4338–4344
14. Yan F, Huo M, Wang M, Yao H, Zhang LYJ (2009) Synthesis of a novel asymmetric gemini surfactant and pH-controlled vesicle aggregation. Chem Lett 38:316–317
15. Huang X, Cao M, Wang J, Wang Y (2006) Controllable organization of a carboxylic acid type gemini surfactant at different pH values by adding copper (II) ions. J Phys Chem B 110:19479–19486
16. Yin H, Huang J, Gao Y, Fu H (2005) Temperature-controlled vesicle aggregation in the mixed system of sodium n-dodecyl sulfate/n-dodecyltributylammonium bromide. Langmuir 21:2656–2659
17. Yin H, Lin Y, Huang J, Ye J (2007) Temperature-induced vesicle aggregation in catanionic surfactant systems: the effects of the headgroup and counterion. Langmuir 23:4225–4230
18. Menger FM, Peresypkin AV (2003) Strings of vesicles: flow behavior in an unusual type of aqueous gel. J Am Chem Soc 125:5340–5345
19. Dreiss CA (2007) Wormlike micelles: where do we stand? Recent developments, linear rheology and scattering techniques. Soft Matter 3:956–970
20. Xie D, Zhao J, You Y (2013) Construction of a highly viscoelastic anionic wormlike micellar solution by carboxylate gemini surfactant with a p-dibenzenediol spacer. Soft Matter 9:6532–6539
21. Xie D, Zhao J (2013) Unique aggregation behavior of a carboxylate gemini surfactant with a long rigid spacer in aqueous solution. Langmuir 29:545–553
22. Israelachvili JN, Mitchell DJ, Ninham BW (1976) Theory of self-assembly of hydrocarbon amphiphiles into micelles and bilayers. J Chem Soc Faraday Trans 2, 72: 1525–1568
23. Evans DF, Ninham BW (1986) Molecular forces in the self-organization of amphiphiles. J Phys Chem 90:226–234
24. Jiang R, Huang YX, Zhao JX, Huang CC (2008) Transformation of vesicles in aqueous two-phase system of an anionic gemini surfactant and a cationic conventional surfactant mixture. Chin J Chem 26:635–639
25. Jiang R, Huang YX, Zhao JX, Huang CC (2009) Aqueous two-phase system of an anionic gemini surfactant and a cationic conventional surfactant mixture. Fluid Phase Equilib 277:114–120